Skin Aging in Long-Lived Naked Mole-Rats Is Accompanied by Increased Expression of Longevity-Associated and Tumor Suppressor Genes

Iqra Fatima[1], Guodong Chen[2], Natalia V. Botchkareva[2], Andrey A. Sharov[2], Daniel Thornton[3], Holly N. Wilkinson[4], Matthew J. Hardman[4], Andreas Grutzkau[5], Joao Pedro de Magalhaes[3], Andrei Seluanov[6,7], Ewan St. J. Smith[8], Vera Gorbunova[6,7], Andrei N. Mardaryev[1,10], Chris G. Faulkes[9,10] and Vladimir A. Botchkarev[2,10]

Naked mole-rats (NMRs) *(Heterocephalus glaber*) are long-lived mammals that possess a natural resistance to cancer and other age-related pathologies, maintaining a healthy life span >30 years. In this study, using immunohistochemical and RNA-sequencing analyses, we compare skin morphology, cellular composition, and global transcriptome signatures between young and aged (aged 3–4 vs. 19–23 years, respectively) NMRs. We show that similar to aging in human skin, aging in NMRs is accompanied by a decrease in epidermal thickness; keratinocyte proliferation; and a decline in the number of Merkel cells, T cells, antigen-presenting cells, and melanocytes. Similar to that in human skin aging, expression levels of dermal collagens are decreased, whereas matrix metalloproteinase 9 and matrix metalloproteinase 11 levels increased in aged versus in young NMR skin. RNA-sequencing analyses reveal that in contrast to human or mouse skin aging, the transcript levels of several longevity-associated (*Igfbp3, Igf2bp3, Ing2*) and tumor-suppressor (*Btg2, Cdkn1a, Cdkn2c, Dnmt3a, Hic1, Socs3, Sfrp1, Sfrp5, Thbs1, Tsc1, Zfp36*) genes are increased in aged NMR skin. Overall, these data suggest that specific features in the NMR skin aging transcriptome might contribute to the resistance of NMRs to spontaneous skin carcinogenesis and provide a platform for further investigations of NMRs as a model organism for studying the biology and disease resistance of human skin.

Journal of Investigative Dermatology (2022) **142,** 2853–2863; doi:10.1016/j.jid.2022.04.028

INTRODUCTION

The skin forms an interface between the external environment and internal milieu that protects mammalian organisms against uncontrolled water loss and numerous environmental stressors, including mechanical injury, UV irradiation, thermal/chemical insults, harmful microorganisms, and viruses (Chuong et al., 2002; Larsen et al., 2020; Menon and Kligman, 2009; Slominski et al., 2012). To fulfill such complex functions, different cell lineages of epithelial, mesenchymal, and neuroectodermal origin interact with each other and form a robust and plastic biological system capable of maintaining homeostasis and responding efficiently to environmental challenges (Rognoni and Watt, 2018).

Similar to other organs, the skin undergoes both intrinsic (chronological) and extrinsic (environmental) aging associated with changes in visual appearance and loss of functional capacity and regenerative potentials (Rittié and Fisher, 2015; Yaar et al., 2002). Major age-related changes in the skin include wrinkling, dryness, pigmentation abnormalities, and the development of a variety of benign neoplasms (Yaar et al., 2002). Microscopically, skin aging is accompanied by the decrease of epidermal thickness and keratinocyte (KC) proliferation, decline in the number of melanocytes and Langerhans cells, flattening of the dermal–epidermal junction, decline of dermal volume and cellularity, fragmentation of collagen and elastic fibers, decrease of dermal blood/lymphatic vessels, and decrease in cutaneous innervation and sensory perception (Rittié and Fisher, 2015; Yaar et al., 2002).

At the molecular level, aging of the epidermis is accompanied by alterations of gene expression in the KC-specific

[1]*Centre for Skin Sciences, Faculty of Life Sciences, University of Bradford, Bradford, United Kingdom;* [2]*Department of Dermatology, Boston University School of Medicine, Boston, Massachusetts, USA;* [3]*Genomics of Aging and Rejuvenation Laboratory, Institute of Life Course and Medical Sciences, Univeristy of Liverpool, Liverpool, United Kingdom;* [4]*Centre for Atherothrombosis and Metabolic Disease, Hull York Medical School, University of Hull, Hull, United Kingdom;* [5]*Deutsches Rheuma-Forschungszentrum Berlin, Institute of the Leibniz Association, Berlin, Germany;* [6]*Department of Biology, School of Arts & Sciences, University of Rochester, Rochester, New York, USA;* [7]*Department of Medicine, School of Medicine and Dentistry, University of Rochester, Rochester, New York, USA;* [8]*Department of Pharmacology, University of Cambridge, Cambridge, United Kingdom; and* [9]*School of Biological and Behavioural Sciences, Queen Mary University of London, London, United Kingdom*

[10]*These authors contributed equally to this work.*

Correspondence: Vladimir A. Botchkarev, Department of Dermatology, Boston University School of Medicine, 609 Albany Street, Boston, Massachusetts 02118, USA. E-mail: vladbotc@bu.edu

Abbreviations: HA, hyaluronic acid; IGF, insulin GF; KC, keratinocyte; MMP, matrix metalloproteinase; NMR, naked mole-rat; ONMR, old naked mole rat; RNAseq, RNA-sequencing; TSG, tumor suppressor gene; YNMR, young naked mole rat

Received 16 June 2021; revised 26 April 2022; accepted 26 April 2022; accepted manuscript published online 9 June 2022; corrected proof published online 18 August 2022

gene loci, loss of terminal differentiation–associated calcium gradient, decreased lipid synthesis and hyaluronic acid (HA) content, and cytokine imbalance and results in compromised epidermal barrier function (He et al., 2020). Thinning and flattening of the dermal–epidermal junction in aged skin is accompanied by a significant reduction in the levels and distribution of collagens IV/VII/XVII, integrin β4, and laminin-332 (Langton et al., 2016). Dermal changes in aged skin also include fragmentation of both collagen and elastic fibers, a decrease in the levels of major extracellular matrix components (decorin, versican), and upregulation of the matrix metalloproteinase (MMP) 1/3/9 that cleave collagen and elastic fibrils (Cole et al., 2018).

Age-associated alterations in the skin immune system include a decrease in the antigen-presenting and migratory capacities of Langerhans and dendritic cells, resulting in alterations of the barrier immunity and the development of chronic low-grade inflammation (inflammaging) (Pilkington et al., 2021). Accumulation of senescent cells in the aged epidermis and dermis (Gunin et al., 2014; Victorelli et al., 2019; Waaijer et al., 2016) contributes to the inflammaging phenotype owing to their production of proinflammatory cytokines as a part of senescent-associated secretory phenotype (Toutfaire et al., 2017).

There are quite legitimate concerns among many researchers raising the question of whether the mechanisms of aging identified in short-lived mammals, such as mice or rats, adequately reflect the complexity of longevity pathways that regulate aging in long-lived species such as humans (Dammann, 2017). Naked mole-rats (NMRs) (*Heterocephalus glaber*) are long-lived rodents possessing remarkable resistance to spontaneous carcinogenesis, certain noxious stimuli, and hypoxia and maintain a sustained healthy life span for over 30 years (Buffenstein, 2005; Gorbunova et al., 2014; Seluanov et al., 2018; Smith et al., 2020). Comparative genome analyses have revealed that the NMR genome shows higher similarity (93% synteny) to the human genome than that of mice (83%) or rats (80%) (Gladyshev et al., 2011; Kim et al., 2011). Many aspects of the NMR biology have recently been extensively discussed (Braude et al., 2021; Buffenstein et al., 2022), leading to the conclusion that the exceptional resistance of NMRs to aging-associated pathologies is mediated by several mechanisms, including more robust DNA repair and genome stability than in mice, a unique organization of the tumor suppressor *Ink4a/b* locus, production of large amounts of higher-molecular-weight HA with unusual properties, altered insulin GF (IGF) receptor signaling, and increased proteasome activity and protein stability (Brohus et al., 2015; Del Marmol et al., 2021; Evdokimov et al., 2018; Gorbunova et al., 2014; Keyes et al., 2013; Kulaberoglu et al., 2019; MacRae et al., 2015; Rodriguez et al., 2016; Seluanov et al., 2018; Takasugi et al., 2020).

The skin of the NMRs displays distinctive morphological features associated with adaptation of these animals to the subterranean environment: relatively thick epidermis with an unusually thick corneal layer, presence of pigment-containing cells in the dermis, lack of hair follicles on most of the skin (Daly and Buffenstein, 1998; Menon et al., 2019; Thigpen, 1940). However, it is unclear how the NMR skin changes during aging and whether there are any particular features in the NMR skin transcriptome that underlie the remarkable natural resistance of NMRs to spontaneous skin carcinogenesis.

In this manuscript, we show that skin aging in the NMR resembles many features of human skin aging, including histological and biochemical changes in both the epidermis and dermis. However, in contrast to those in human skin, transcripts and proteins of several longevity-associated and tumor suppressor genes (TSGs) are increased in the NMR skin during aging. These data suggest that these features of the NMR skin aging transcriptome might contribute to the resistance of NMRs to spontaneous skin carcinogenesis, thus reaffirming the potential of the NMR as a model organism for studying both the biology and disease of human skin.

RESULTS

Epidermis of aged NMRs shows decreased thickness, cell proliferation, and reduced expression of the KC differentiation marker COL17A1 and Merkel cells

To assess the impact of aging on NMR skin, we first compared visual appearance, morphological parameters, and expression of established KC differentiation markers between the dorsal skin epidermis of young (aged 2–4.5 years) and aged (aged 19–23 years) animals (Figure 1a). Consistent with data published previously (Daly and Buffenstein, 1998; Tucker, 1981), the dorsal skin of NMRs has a wrinkled and saggy macroscopic appearance and a lack of any skin appendages (Figure 1b). Single unpigmented hairs are only visible in the lateral part of the body, whereas vibrissa hairs are numerous on the facial skin (Figure 1a). In contrast to the skin of young NMRs (YNMRs), the skin of old NMRs (ONMRs) appeared thinner, more translucent, and less pigmented (Figure 1b). Histologically, the dorsal skin of YNMRs presented a relatively thick multilayered epidermis with a thick stratum corneum (Menon et al., 2019), whereas in ONMRs, the epidermal thickness was significantly reduced (Figure 1c). The majority of Ki-67+ cells were located in the basal epidermal layer, whereas their number was markedly decreased in ONMRs versus that in YNMRs (Figure 1d).

In the NMR epidermis, keratin 14 expression was mainly confined to the basal layer, whereas keratin 10 and loricrin were seen in the spinous and granular layers, respectively (Figure 1e–g). However, the immunofluorescence intensity for all the three markers as well as for p63 transcription factor, a master regulator of epidermal development and differentiation (Koster et al., 2007), was significantly decreased in the epidermis of ONMRs compared with that of YNMRs (Figure 1e–h).

The expression of COL17A1, an established marker of epidermal aging (Liu et al., 2019), was also decreased in basal epidermal KCs and dermal–epidermal basement membrane of ONMRs compared with those of YNMRs (Figure 1i). In addition, the number of keratin 20+ Merkel cells, specialized sensory cells involved in mechanotransduction (Jenkins et al., 2019), was significantly lower in the epidermis of ONMRs than in that of YNMRs (Figure 1j). However, epidermal Caspase 3+ apoptotic cells did not reveal any differences in their number between YNMRs and ONMRs (Supplementary Figure S1a).

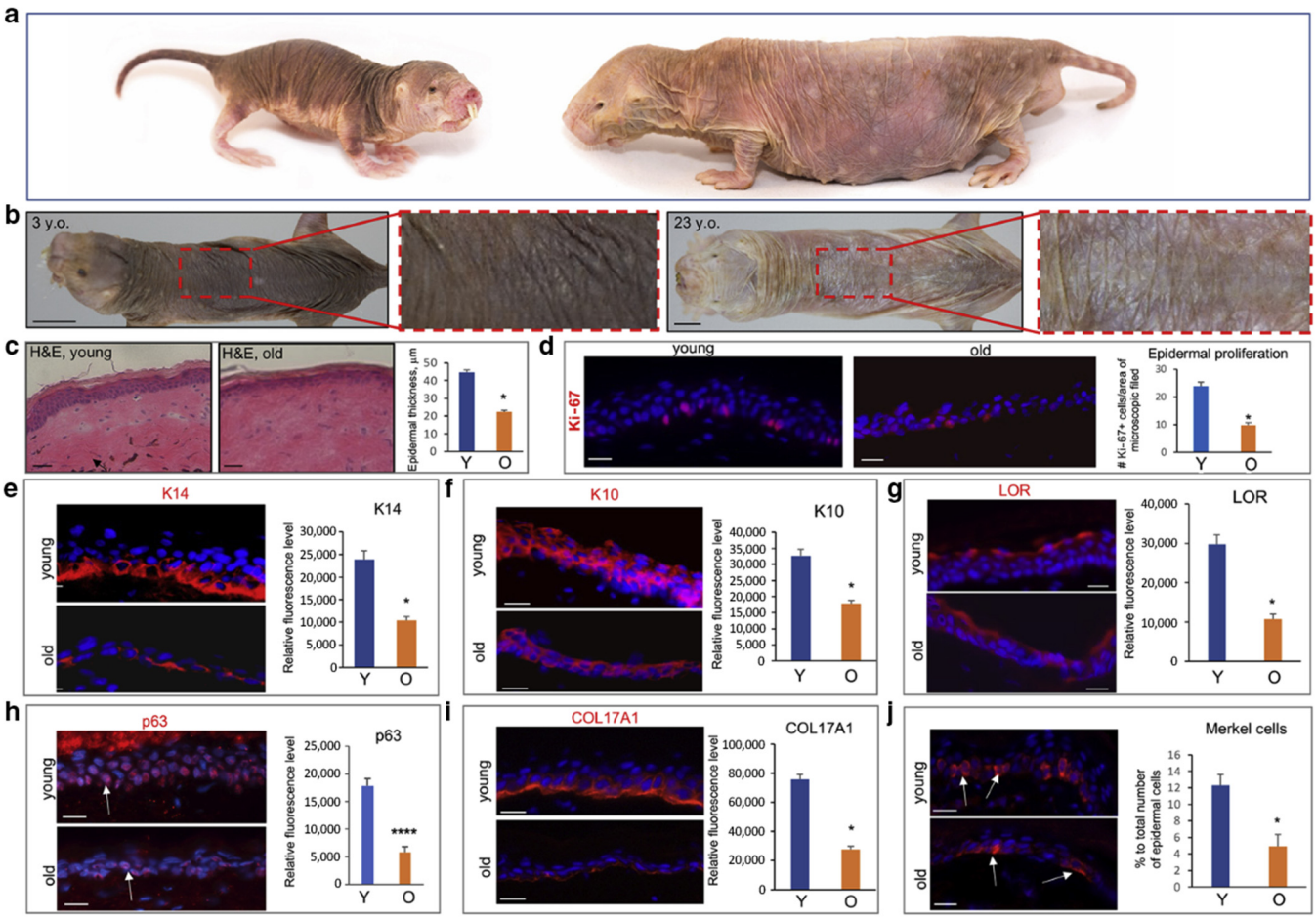

Figure 1. Visual appearance of the skin- and age-related changes in the epidermis of NMRs. **(a,b)** Images of the skin in animals aged 3 and 23 years. Note the more translucent and less pigmented dorsal skin in aged NMR. (**c**) H/E staining of the young and old skin: the presence of the dermal pigment in young skin and significantly reduced epidermal thickness in old animals. (**d**) Significant decrease in Ki-67+ cells in aged versus young NMRs. (**e–g**) Significantly decreased immunofluorescence intensity of (**e**) K14 in the basal layer, (**f**) K10 in the spinous layer, and (**g**) LOR in the granular layer in the epidermis of old NMRs. (**h**) Significant decrease in the immunofluorescence intensity of p63 in epidermal keratinocytes of old versus young NMRs. (**i**) Significant decline in the expression of COL17A1 in basal epidermal keratinocytes and dermal–epidermal basement membrane of old animals. (**j**) Significant decrease in the number of K20+ Merkel cells in the epidermis of old NMRs (arrows). Data are expressed as mean ± SD. $^*P < 0.05$ with Student's *t*-test. Bars = 1 cm for **b**, 50 um for **c**, and 25 um for **d–j**. Y denotes young animals, and O denotes old animals. K, keratin; LOR, loricrin; NMR, naked mole-rat; y.o., year old.

Age-associated changes in the NMR dermis include decreased COL1A1 expression, an increase in MMP9 and MMP11, and loss of melanocytes

The NMR epidermis forms invaginations or buds elongating into the dermis (Tucker, 1981). Their numbers were significantly decreased in ONMRs, contributing to age-associated flattening of the epidermal–dermal interface (Figure 2a). Similar to the elastic fibers in the human skin (Langton et al., 2010), fibrillin 2–enriched elastic fibers in the papillary dermis of NMRs formed candelabra-like cascades ascending toward the dermal–epidermal junction and epidermal buds, whereas their number was not changed between YNMRs and ONMRs (Figure 2b). Moreover, the distribution of dermal elastic fibers and elastin expression levels were quite similar in the dermis of YNMRs and ONMRs (Supplementary Figure S1b).

COL1A1, an important component of the mature collagen fibers providing tensile strength to the skin (Cole et al., 2018), was broadly expressed in the papillary and reticular dermis of YNMRs (Figure 2c). In ONMRs, dermal COL1A1 expression declined compared with that in YNMRs (Figure 2c), whereas the expression levels of COL3A1, a marker of immature collagen fibers, did not show significant differences between YNMRs and ONMRs (Supplementary Figure S1c).

MMPs promote age-associated extracellular matrix remodeling (Cole et al., 2018). Immunohistochemistry revealed a marked increase of MMP9 and MMP11 immunofluorescence in the dermis of ONMRs compared with that of YNMRs (Figure 2d and Supplementary Figure S1e). However, MMP1 levels did not show significant changes between ONMRs and YNMRs (Supplementary Figure S1d).

The NMR extracellular matrix contains HA, which unlike mouse HA forms highly folded structures that may contribute to the elasticity of NMR skin (Kulaberoglu et al., 2019). Moreover, HA appears to be present in larger amounts and has a higher molecular weight in NMRs than in mice or guinea pigs (Del Marmol et al., 2021; Keyes et al., 2013). However, HABP immunostaining used previously for analyses of the HA content in the skin (Kulaberoglu et al., 2019) and the HA receptor CD44 levels did not show any differences between the dermis of YNMRs and that of ONMRs (Figure 2e and f).

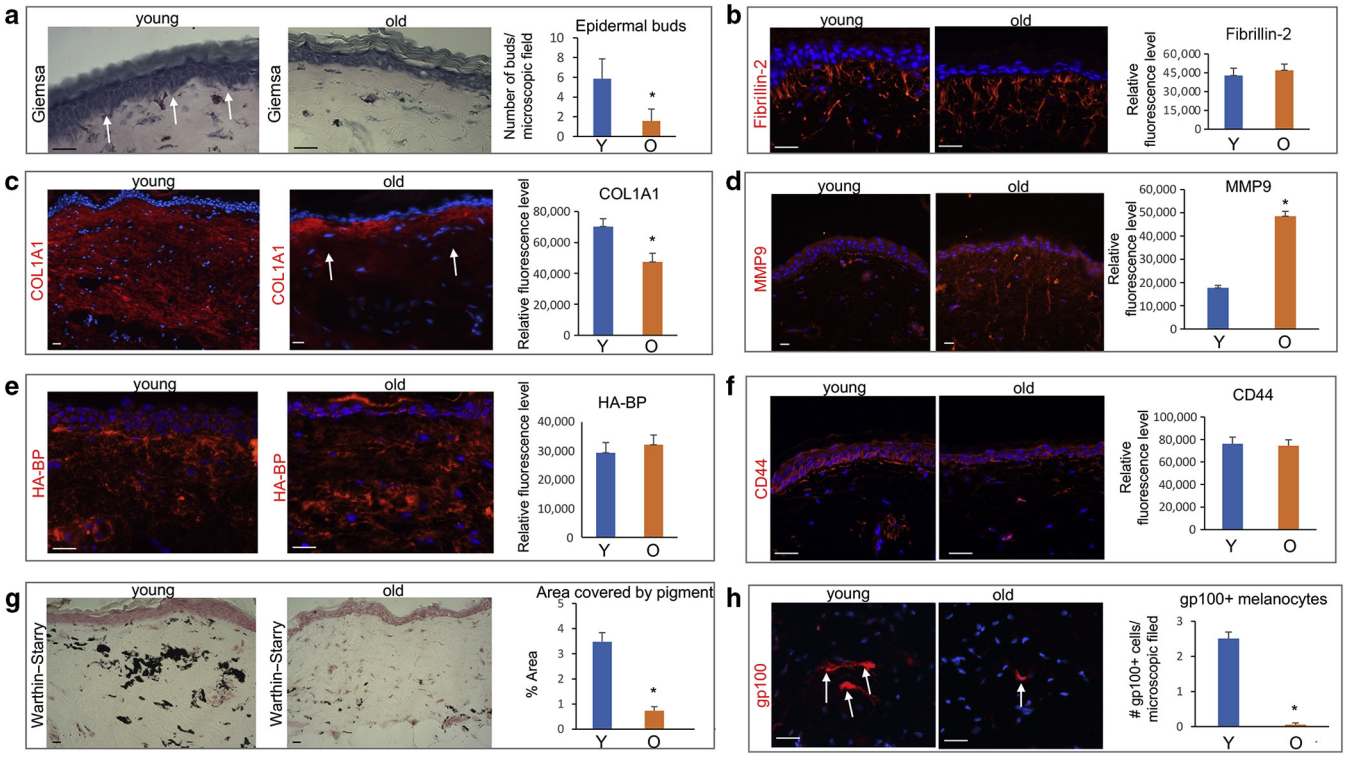

Figure 2. Age-associated changes in the NMR dermis. (a) Significantly reduced number of epidermal buds elongating into the dermis (arrows) in the aged NMR skin. **(b)** A similar distribution of fibrillin 2–positive fibers in young and old NMRs. **(c)** COL1A1 is broadly expressed in the papillary and reticular dermis of young NMRs, whereas COL1A1 expression is significantly decreased in the reticular dermis in aged skin. **(d)** Significant increase in the MMP9 immunofluorescence intensity in the dermis of old NMRs compared with that in the young animals. **(e)** No differences in the HA-BP–binding pattern or degree of binding between the dermis of young and old NMRs. **(f)** Similar expression of the HA receptor CD44 in the skin of young and old NMRs. **(g)** Warthin–Starry stain shows a dramatic decrease in the melanin-containing areas in the dermis of old compared with that of young NMRs, which is accompanied by a significant decrease in the number of gp100+ pigment-producing dermal melanocytes in the **(h)** dermis of aged animals (arrows). Data are expressed as mean ± SD. $*P < 0.05$ with Student's *t*-test. Bars = 25 μm. Y denotes young animals, and O denotes old animals. HA, hyaluronan; HA-BP, hyaluronan-binding protein; MMP, matrix metalloproteinase; NMR, naked mole-rat.

One of the characteristic features of the NMR dorsal skin is the presence of a large number of pigmented melanocytes in the dermis (Daly and Buffenstein, 1998). Consistently with the visual loss of skin pigmentation in ONMRs (Figure 1a), Warthin–Starry staining of melanin (Joly-Tonetti et al., 2016) revealed a dramatic decrease in the areas covered by the pigment in the dermis of ONMRs compared with that of YNMRs (Figure 2g). In addition, the number of melanocytes expressing gp100 that is expressed in melanogenically active melanocytes (Watt et al., 2013) was markedly reduced in the dermis of ONMRs (Figure 2h).

Aged NMR skin exhibits decreased CD3E T cells, major histocompatibility complex class II antigen-presenting cells, and mast cells and an increase of senescent cells

To characterize the changes in the skin immune system occurring during aging in NMRs, we used a panel of primary antibodies established for analysis of immune cell markers in NMRs (Shebzukhov et al., 2019). Comparative studies of the immune cell markers revealed that ONMRs show a significant decrease in the number of CD3E-positive T cells and major histocompatibility complex II–positive cells in the epidermis and dermis (Figure 3a and b and Supplementary Figure S1f). A quantitative analysis of CD8+ cells and CD11B+ (macrophages) cells in the dermis did not reveal any differences between ONMRs and YNMRs (Figure 3c and d). In contrast, the number of mast cells was significantly lower in the dermis/subcutis of ONMRs than in young animals (Supplementary Figure S1g).

The presence of senescent cells in the skin of NMRs was previously reported (Zhao et al., 2018). Senescence-associated β-galactosidase staining revealed a significant increase in the number of senescence-associated β-galactosidase–positive cells in the aged epidermis and only a tendentious increase in the dermis of ONMRs, which did not reach statistical significance ($P = 0.082$) (Figure 3e). The increase in the number of senescent cells in the ONMR skin was accompanied by the elevated expression of $p16^{INK4a}$ transcript as an important marker of senescent cells (Ressler et al., 2006) that was determined by quantitative real-time polymerase chain reaction (qRT-PCR) in full-thickness skin samples (Supplementary Figure S1h). However, the expression of both $p15^{INK4b}$ and $pALT^{INK4a/b}$ transcripts remained unaltered between old and young skin (Supplementary Figure S1h).

Transcriptome analysis of NMR aging skin reveals changes in the expression of extracellular matrix–associated genes, components of the IGF signaling pathway, regulators of glucose metabolism, and cell proliferation

To further characterize the changes occurring in the NMR skin during aging on the molecular level, RNA-sequencing (RNAseq) analyses of the full-thickness skin of animals aged

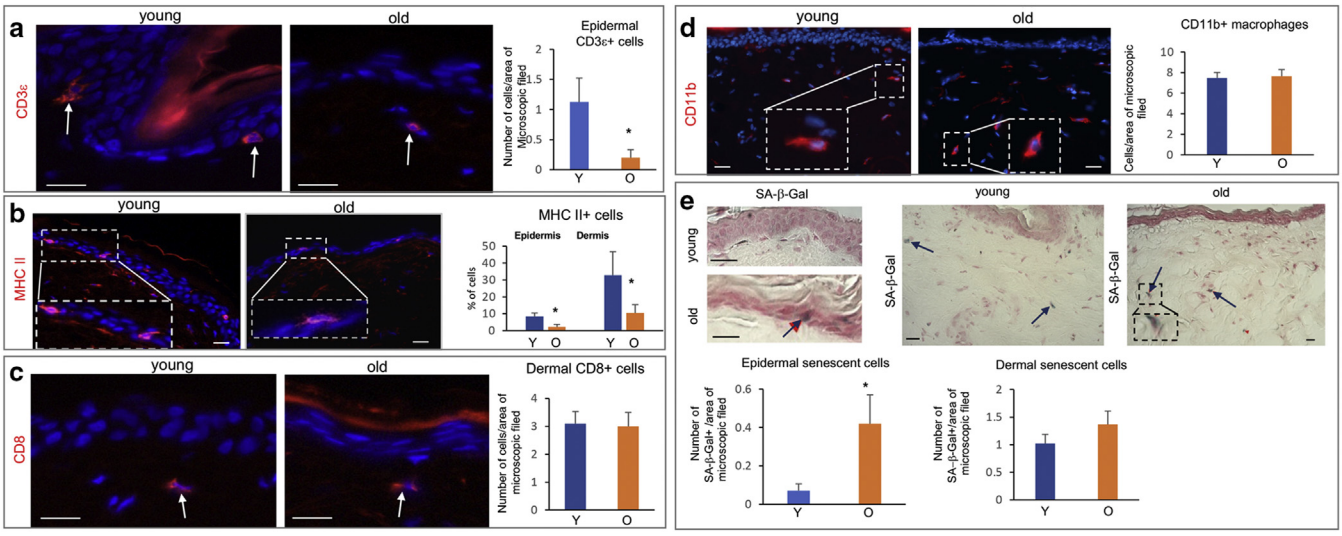

Figure 3. Aging-associated changes in the number of immune and senescent cells in the NMR skin. (a) Significant decrease in the number of CD3ε+ T cells in the epidermis of old NMRs. **(b)** Significant decrease in the number of MHC II+ cells detected by an anti-27E7 antibody in the epidermis and dermis of old NMRs. **(c)** No changes in the number of CD8+ cells in the dermis of aged versus young NMRs (arrows). **(d)** The number of dermal CD11b+ macrophages is similar in the young and old NMRs. **(e)** Significant increase in the number of senescent SA-β-Gal+ cells (arrow) in the epidermis of old NMRs. A tendentious but not significant increase in the number of SA-β-Gal+ cells (arrows) in the aged dermis ($P = 0.082$). Data are expressed as mean ± SD. *$P < 0.05$ with Student's *t*-test. Bars = 25 μm. Y denotes young animals, and O denotes old animals. MHC, major histocompatibility complex; NMR, naked mole-rat; SA-β-Gal, senescence-associated β-galactosidase.

4 years and 19 years were performed and revealed significant (two-fold and higher) changes in the expression of 768 genes between the skin of YNMRs and ONMRs (Figure 4a and b). Overall, RNAseq data were concordant with our histomorphology/immunohistochemistry results (Figures 1 and 2 and Supplementary Table S3) and identified the decline in expression of dermal collagen genes (*Col1a1, Col1a2)*, genes encoding T-cell and Langerhans cell markers (*Thy1, Cd3d, Cd207),* as well as genes encoding melanocyte/melanogenesis-associated markers (*Dct, Tyrp1, Slc24a5*) in ONMR skin compared with those in YNMR skin (Figure 4c and Supplementary Tables S2 and S3). Consistent with the immunohistochemistry results (Figure 2d and Supplementary Figure S1d), RNAseq analyses also detected an increase in *Mmp9* and *Mmp11* gene expression in ONMR skin versus in YNMR skin (Figure 4c and Supplementary Table S1).

Interestingly, among the group of extracellular matrix–associated genes differentially expressed in the ONMR skin, we found a marked downregulation of numerous collagen genes, including *Col1a1, Col1a3, Col3a1*, and genes encoding the enzymes involved in collagen synthesis (*Pcolce, Pcolce2)* and fibrillogenesis (*Cthrc1, Sparc*) (Figure 4a–c and Supplementary Table S2). In addition, several genes encoding extracellular matrix–degrading enzymes (*Mmp11, Mmp9, Pm20d2, Adamts5*) were upregulated in the skin of ONMRs compared with the skin of YNMRs, whereas *Mmp27* and *Mmp19* were downregulated (Figure 4a–c and Supplementary Tables S1 and S2). Although it is known that MMP9 and MMP11 can be processed by other MMPs, such as MMP2 (Bonnans et al., 2014), we observed no difference in expression levels of *Mmp2* as well as of transcript of another enzyme (*Furin*) involved in the MMP processing/cleavage between ONMR and YNMR skin (data not shown).

A group of genes involved in the regulation of glucose metabolism included *Pdk4*, which encodes pyruvate dehydrogenase kinase 4 promoting a switch from oxidative energy metabolism to glycolysis (Stacpoole, 2012). *Pdk4* was strongly upregulated in the skin of ONMRs as well as the *Pck1* gene, a critical regulator of gluconeogenesis, *Acacb* encoding a key enzyme in fatty acid synthesis, and *Slc2a6* encoding the glucose transporter GLUT6 (Barron et al., 2016).

IGF signaling is implicated in the control of longevity (Brohus et al., 2015), including skin aging (Lewis et al., 2010). RNAseq analysis revealed that expression of *Igf1* was decreased in ONMR skin compared with that in YNMRs, whereas the expression levels of transcripts for the IGF1/2 binding proteins *Igfbp3* and *Igf2bp3* were increased (Supplementary Tables S1 and S2).

The group of genes involved in cell cycle regulation that show differences in expression between ONMR and YNMR skin included cyclin-dependent kinase inhibitors (*Cdkn1a, Cdkn2c*) and a member of the antiproliferative BTG/TOB family (*Btg2*), whose expression patterns in aged skin were upregulated (Figure 4c and Supplementary Table S1). These changes were accompanied by decreased expression of genes positively regulating cell proliferation, including *Pcna, Ccne1* gene encoding cyclin E1, centromere-associated protein genes (*Cenph, Cenpm, Cenpn, Cenpw, Cenpx*), and genes controlling mitotic cell division (*Ncapg2, Pole1, Tk1)* and cell cycle–associated transcription machinery (*E2f1*) (Figure 4c and Supplementary Table S2). The significant increase of CDKN1A, BTG2, and TOB1 at the protein level in the NMR aged epidermis was further confirmed by quantitative immunofluorescence analysis (Supplementary Figure S3). These data were consistent with the results showing the decrease of epidermal proliferation in ONMRs compared with that in YNMRs (Figure 1d).

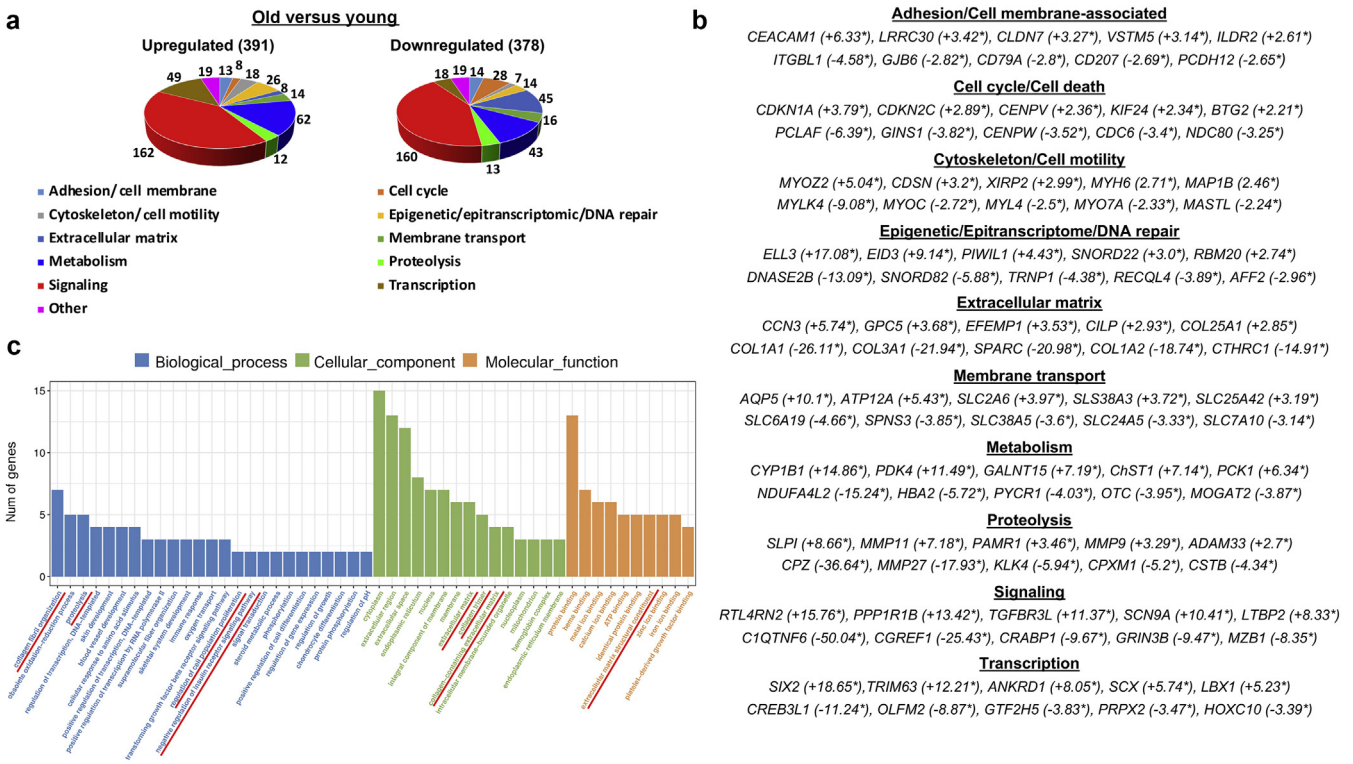

Figure 4. RNAseq analyses of the age-associated changes in the cutaneous NMR transcriptome. (a) Functional annotation of the differentially expressed genes based on Qiagen Ingenuity Pathway Analysis database and manually curated functional gene subcategories. **(b)** A list of five top differentially expressed genes in each functional group (fold-change expression values are indicated by asterisks). **(c)** GO enrichment analysis showed significant over-representation of the extracellular matrix–associated genes, components of the IGF signaling pathway, and regulators of glucose metabolism and cell proliferation. GO, Gene Ontology; IGF, insulin GF; NMR, naked mole-rat; RNAseq, RNA sequencing.

Species-specific differences in aging transcriptomes hint at a potential contribution to longevity and cancer resistance in NMRs

To correlate the age-associated changes in the NMR skin transcriptome to human or mouse skin aging, we compared our data with four publicly available RNAseq skin aging datasets obtained from either full-thickness skin or epidermis of human and mouse skin (young vs. aged) (Aramillo Irizar et al., 2018; Barth et al., 2019; Ge et al., 2020; Raddatz et al., 2013). This analysis revealed that only a relatively small number of genes whose expression was changed in the ONMR skin (11.7% of upregulated and 16.9% of downregulated genes) showed a similar trajectory in the aged human and mouse skin. Surprisingly, most genes differentially expressed during NMR skin aging were not changed in either human or mouse skin aging, whereas a small number of differentially expressed genes (11.0 and 14.5% of upregulated and downregulated genes, respectively) in the NMR aging transcriptome showed opposite dynamics to those of aged human or mouse skin (Supplementary Figure S2 and Supplementary Tables S4 and S5).

To further correlate the relevance of age-associated changes in the NMR cutaneous transcriptome to other age-related datasets, we used the Human Ageing Genome Resource database platform (Tacutu et al., 2018). We found that 113 genes differentially expressed in ONMR skin (16.3% of the upregulated and 12.9% of downregulated genes, defined as NMR aging signature genes) were present in one or more Human Ageing Genome Resource datasets (Figure 5a and Supplementary Table S6). According to the Human Ageing Genome Resource databases, substantially more NMR aging signature genes were relevant to human aging than to animal aging (33 vs. 12, respectively), whereas eight NMR genes belonged to both datasets (GeneAgeHuman and GeneAgeModel) (Supplementary Table S6).

In ONMR skin, RNAseq detected elevated expression of *Fos* and *Jun* (Supplementary Table S1), encoding essential components of the activator protein-1 transcription factor, stimulating the expression of MMPs during UV-induced photoaging in human skin (Rittié and Fisher, 2002, 2015). In addition, among the genes upregulated in ONMR skin was *Igfbp3*, implicated in the control of longevity and counteracting the life-shortening effects of IGF signaling (Martins et al., 2016), as well as antiproliferative genes *Cdkn1a* and *Cdkn2c* (Supplementary Table S6). Protein–protein interaction network analysis performed using the STRING (search tool for retrieval of interacting genes) software tool (http://string-db.org, vision 11.0) (Crosara et al., 2018) revealed links between the Fos/Jun genes with TSGs *Cdkn1a*/*Cdkn2c*/*Zfp36* upregulated in ONMR skin (Supplementary Figure S4). On the other hand, the longevity-related genes downregulated in ONMR skin formed a network controlling extracellular matrix remodeling, IGF signaling, and DNA replication/cell division (Supplementary Figure S5).

Because NMRs show remarkable resistance to spontaneous carcinogenesis, we intersected the age-associated NMR

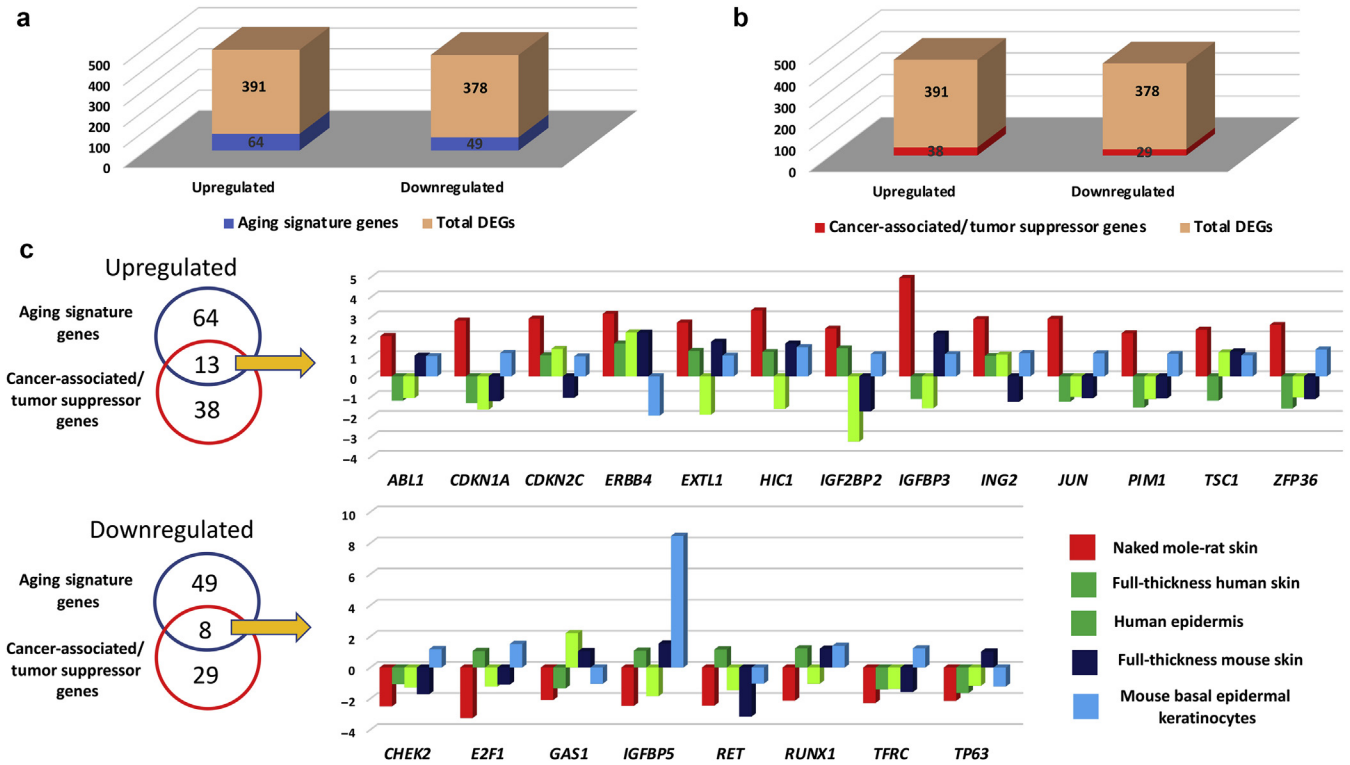

Figure 5. Comparison of age-associated changes in the transcriptome of NMR, human, and mouse skin. (a) The number of DEGs common between the NMR skin aging transcriptome and the HAGR genes (denoted as aging signature genes in this study) relative to the total number of DEGs. **(b)** The number of DEGs common between the NMR skin aging transcriptome and the CGC/TSGene datasets (denoted as cancer signature genes in this study) relative to the total number of DEGs. **(c)** A Venn diagram shows the DEGs in the NMR skin aging transcriptome that are shared with the human HAGR and CGC/TSGene databases. Comparative analyses of gene expression (old vs. young) in the skin of three species: NMR (total skin), human (total skin, epidermis), and mouse (total skin, FACS-sorted basal epidermal keratinocytes). The differences in gene expression are shown as the FPKM fold change. CGC, Cancer Gene Census; DEG, differentially expressed gene; FPKM, fragment per kilobase of exon per million mapped fragment; HAGR, Human Ageing Genome Resource; NMR, naked mole-rat; TSGene, Tumor Suppressor Genes.

transcriptome with the human Cancer Gene Census database (Welcome Sanger Institute/EBI, Hinxton, United Kingdom) (Sondka et al., 2018) and Tumor Suppressor Genes database (University of Texas, Houston, TX). We found that 67 differentially expressed genes in the ONMR skin were present in the Cancer Gene Census/Tumor Suppressor Genes databases, representing the NMR cancer-related/TSG signature genes (Figure 5b). Interestingly, this group of genes contained not only inhibitors of the IGF pathway but also inhibitors of the Jak/signal transducer and activator of transcription (*Sosc3)* and Wnt (*Sfrp1* and *Sfrp5)* pathways (Supplementary Table S7).

After the merging of the longevity-associated and cancer-related genes/TSG, we found 21 common genes seen in the Human Ageing Genome Resource and Cancer Gene Census/Tumor Suppressor Genes databases (Figure 5c), thus demonstrating their relevance to both longevity and cancer development/resistance. The group of the longevity/cancer-related/TSG signature genes upregulated in ONMR skin (Figure 5c) included cell cycle inhibitors *Cdkn1a/Cdkn2c* (Winkler, 2010), tumor suppressor *Hic1* gene encoding transcriptional repressor downregulated in many cancers (Rood and Leprince, 2013), as well as *Tsc1* gene mutated in tuberous sclerosis complex disease characterized by formation of tumor-like lesions (hamartomas) in the skin (Rosset et al., 2017). In addition, the expression of *Zfp36* gene encoding RNA-binding protein tristetraprolin inhibiting the formation of squamous cell carcinomas (Assabban et al., 2021) was upregulated in ONMR skin (Figure 5c). In addition, expression of *Dnmt3a* regulating de novo DNA methylation (Parry et al., 2021) increased in ONMR skin compared with that in YNMR skin (Supplementary Table S7).

Among the longevity-associated/cancer-related genes downregulated in ONMR skin (Figure 5c) were proto-oncogene *Ret*, transcription factor *E2f1* promoting cell proliferation and upregulated in chemically induced squamous cell carcinomas (Balasubramanian et al., 1999), and *Tp63* downregulated in human skin during aging (Figure 5c). Protein–protein interaction network of the cancer-related genes/TSGs revealed additional links between a group of tumor suppressors (*Btg2, Sfrp1, Socs3, Thbs1*) and oncogenes (*Abl1, Flt3, Kras, Sparc*) as well as between DNA methyltransferase *Dnmt3a,* components of the fibroblast GF signaling pathway *Flt3/Fgfr4*, and longevity-related *Tp63* (Supplementary Figure S6).

The comparative analyses of the longevity-associated/cancer-related/TSG signature genes in the NMR aging transcriptome with human or mouse skin aging datasets (Aramillo Irizar et al., 2018; Barth et al., 2019; Ge et al., 2020; Raddatz et al., 2013) revealed that none of the 13 genes of this category upregulated in ONMR skin were significantly elevated in aged human or mouse skin, whereas the

expression of only one of eight genes downregulated in ONMR skin showed similar changes in human or mouse skin (Figure 5c and Supplementary Tables S6 and S7). These data suggest that age-associated changes in the cancer-related NMR transcriptome show unique features that may underlie the remarkable resistance of NMRs to spontaneous skin carcinogenesis.

DISCUSSION

In this report, we provide evidence that skin aging in NMRs shows many features similar to those of the aging process in human skin, including (i) a decrease in epidermal thickness, KC proliferation, and expression of epidermal keratins; (ii) a decline in the number of Merkel cells and increase of senescent cells in the epidermis; (iii) flattening of the epidermal/dermal border, decrease in expression levels of dermal collagens, and upregulation of MMP9 and MMP11; (iv) loss of skin pigmentation and decline in the number of dermal melanocytes; and (v) decline in the number of epidermal/dermal T cells and antigen-presenting cells.

Our data showing morphological and biochemical changes in the skin of ONMRs aged 19–23 years appears to be quite different from the data obtained from animals aged 11 years (Savina et al., 2022) and show that skin aging in NMRs occurs during the last trimester of life. Age-associated changes in the NMR epidermis are consistent with a decline in the expression of the p63 transcription factor controlling KC proliferation and differentiation and preventing premature skin aging (Botchkarev and Flores, 2014; Koster et al., 2007; Su et al., 2009). Signaling/transcription factor–regulated and epigenetic mechanisms operate in concert in controlling epidermal differentiation (Ahmed et al., 2014; Botchkarev, 2017; Botchkarev et al., 2012; Fessing et al., 2011; Kouwenhoven et al., 2015; Mardaryev et al., 2016; Qu et al., 2019; Rapisarda et al., 2017). Skin aging in NMRs is accompanied by accumulation of DNA methylation at specific aging-associated differentially methylated CpGs (Horvath et al., 2022; Lowe et al., 2020). In this context, upregulation of genes encoding DNA methyltransferase *Dnmt3a* and methyl-CpG binding protein *Mecp2* (Supplementary Table S1) might contribute to the changes in aging-associated methylome and gene transcription in the skin of ONMRs.

Similar to human skin (Waaijer et al., 2018, 2012), aged NMR skin also shows an increase in the number of senescent cells associated with the upregulation of $p16^{INK4a}$ in the skin. Senescent cells are present in the NMR skin, and NMR dermal fibroblasts are more resistant to induction of stress-induced premature senescence than mouse fibroblasts (Zhao et al., 2018). In aging human skin, senescent cells produce proinflammatory cytokines and contribute to cutaneous inflammaging (Pilkington et al., 2021; Toutfaire et al., 2017). However, detailed transcriptome/proteome analyses of the distinct cell lineages (epithelial, mesenchymal, immune/vascular, pigment, etc.) are required to define the contribution of the senescent cells and their secretory products to the development of age-associated changes in the NMR skin, including cutaneous immune surveillance and inflammatory response.

Despite their remarkable longevity, NMRs also exhibit a potent resistance to spontaneously developing cancers (Seluanov et al., 2018), with a lack of any reported skin cancer incidence, including basal/squamous cell carcinomas and malignant melanomas (Delaney et al., 2013). Our immunohistochemical data showing a lack of decline in the levels of HA and CD44 receptor in aged NMR skin suggest that cytoprotective and anticancer properties of HA (Keyes et al., 2013; Takasugi et al., 2020) are likely not compromised during aging. Comparative transcriptome analyses reveal that in contrast to human or mouse skin aging, skin aging in NMRs is accompanied by upregulation of several classes of TSGs: secreted inhibitors of the IGF, Jak/signal transducer and activator of transcription and Wnt signaling pathways (*Igfbp3, Igf2bp2, Socs3, Sfrp1, Sfrp5)*, cell cycle inhibitors (*Btg2, Cdkn1a, Cdkn2c)*, transcriptional repressor *Hic1*, RNA-binding protein *Zfp36* and epigenetic regulators (*Dnmt3a, Mecp2*). We speculate that together with other longevity-associated genes, these genes form a multilevel regulatory network mediating cancer resistance in the NMR skin.

Undoubtedly, further analyses are required to fully understand the roles of signaling/transcription factor–mediated and epigenetic regulatory mechanisms controlling the age-associated increase in the expression of the longevity-associated genes and TSGs as well as the downregulation of cancer-related genes in the skin of NMRs. Furthermore, age-associated changes in the NMR cutaneous transcriptome need to be correlated with the proteome and protein activity owing to post-transcriptional and post-translational modifications (Buccitelli and Selbach, 2020). These analyses will help to define the unique features of the NMR skin aging transcriptome that might contribute to the resistance NMRs exhibit to spontaneous skin carcinogenesis.

Identification of these mechanisms and their relevance to human skin aging might be beneficial for developing novel approaches for the management of age-associated skin conditions in human, including skin cancer. Taken together, these data provide a platform for further exploration of NMRs as an innovative model organism for studying the biology of human skin and serve as the starting point in the identification of novel mechanisms mediating skin resistance to age-associated pathologies in these unique mammals.

MATERIALS AND METHODS

Animals and tissue collection

All experiments were conducted in accordance with the United Kingdom Animal (Scientific Procedures) Act 1986 Amendment Regulations 2012 under a Project Licenses granted to AM (University of Bradford, Bradford, United Kingdom) and to ESJS (University of Cambridge, Cambridge, United Kingdom) by the Home Office. Animals were maintained in a custom-made caging system with conventional mouse/rat cages connected by different lengths of tunnel. The room was warmed to 28 °C; 50–60% humidity levels were maintained; and bedding, nesting material, and water-enriched food were provided. Four young adult NMRs (aged 3–4.5 years) and three aged NMRs (aged 19–23 years) of both sexes were used in this study. Samples were collected from the dorsal skin, covered in Tissue-Tek medium (VWR International, Poole, United Kingdom),

snap frozen in liquid nitrogen, and stored in a −80 °C freezer (Botchkarev et al., 1999, 1998).

Histology, histomorphometry, and immunohistochemistry

For histology, 10 um cryosections were fixed in 4% paraformaldehyde followed by hematoxylin/eosin staining or by Giemsa staining for mast cell visualization or by the modified Warthin–Starry staining for melanin detection (Joly-Tonetti et al., 2016). To detect senescent cells (Dimri et al., 1995), senescence-associated β-galactosidase staining kit (Cell Signaling Technology, Danvers, MA) was used. The number of mast cells and senescent cells as well as semiautomated skin pigmentation analysis were performed per ×200 microscopic field using ImageJ software (NIH, Bethesda, MD).

For immunofluorescence, 10 um cryosections were fixed and incubated with primary antibodies (Supplementary Table S8), followed by application of the secondary antibodies, as described previously (Botchkareva et al., 1999; Müller-Röver et al., 1998; Sharov et al., 2003). Quantification of immunofluorescence intensity or corrected total cell fluorescence was determined using ImageJ software, as described previously (Rapisarda et al., 2017). Statistical analysis was performed using unpaired Student's *t*-test; differences were deemed significant if $P < 0.05$.

RNAseq, qRT-PCR, and bioinformatics analyses

Total RNA was extracted from full-thickness dorsal skin samples obtained from young and old animals (skin aged 4 years, n = 2; skin aged 19 years, n = 2) and purified using Direct-zol RNA purification kit (Zymo Research, Irvine, CA) followed by DNAse treatment. Integrity of RNA was assessed on 2100 Bioanalyzer Instrument (Agilent Technologies, Santa Clara, CA); only samples with RNA integrity number factor >7.5 were used for next-generation sequencing library preparation. For RNAseq, approximately 10 μg of total RNA was used to remove ribosomal RNA according to the manuscript of the Epicentre Ribo-Zero Gold Kit (Illumina, San Diego, CA). The pair-end 2 × 150 bp sequencing was performed on an Illumina Hiseq 4000 platform in the LC Sciences (Houston, TX).

qRT-PCR was performed with iQ SYBR Green Supermix (Bio-Rad Laboratories, Hercules, CA), as described previously (Mardaryev et al., 2016, 2014). The primer sequences (Supplementary Table S9) were obtained from previously published datasets (Tian et al., 2015). Differences between samples were calculated on the basis of the Ct (ΔΔCt) method and normalized to β-actin. Statistical analysis was performed using unpaired Student's *t*-test.

A detailed description of the bioinformatics and protein–protein interaction network analyses is provided in Supplementary Materials and Methods.

Data availability statement

Datasets related to this article can be found at https://www.ncbi.nlm.nih.gov/geo/query/acc.cgi?acc=GSE200736, hosted at Gene Expression Omnibus (accession number GSE200736).

ORCIDs

Iqra Fatima: http://orcid.org/0000-0003-0610-5797
Guodong Chen: http://orcid.org/0000-0001-9399-9252
Natalia V. Botchkareva: http://orcid.org/0000-0002-5202-6822
Andrey A. Sharov: http://orcid.org/0000-0002-7240-304X
Daniel Thornton: http://orcid.org/0000-0002-4994-2942
Holly N. Wilkinson: http://orcid.org/0000-0002-8453-7264
Matthew J. Hardman: http://orcid.org/0000-0002-6423-5074
Andreas Grutzkau: http://orcid.org/0000-0001-6490-2992
Joao Pedro de Magalhaes: http://orcid.org/0000-0002-6363-2465
Andrei Seluanov: http://orcid.org/0000-0003-3400-538X
Ewan St. J. Smith: http://orcid.org/0000-0002-2699-1979
Vera Gorbunova: http://orcid.org/0000-0001-8979-0333
Andrei N. Mardaryev: http://orcid.org/0000-0002-7826-5506
Chris G. Faulkes: http://orcid.org/0000-0002-5228-9075
Vladimir A. Botchkarev: http://orcid.org/0000-0002-5212-5353

CONFLICT OF INTEREST

The authors state no conflicts of interest.

ACKNOWLEDGMENTS

Authors thank L. Faulkes for help in the preparation of the naked mole rat images for this manuscript. This study was supported in part by the grants from the National Institute of Arthritis and Musculoskeletal and Skin Diseases, United States to VAB, AAS, and VG (R61AR078093); National Institute on Aging, United States to VG and AS; Dunhill Medical Trust, United Kingdom (RPGF2002188) to ESJS. Human Ageing Genome Resource is supported by a Biotechnology and Biological Sciences Research Council, United Kingdom (BB/R014949/1) grant to JPEM. AG was supported by the Leibniz Science Campus Chronic Inflammation, Germany (to AG) (www.chronische-entzuendung.org).

AUTHOR CONTRIBUTIONS

Conceptualization: VAB, CGF, ANM; Data Curation: VAB, CGF, ANM; Formal Analysis: IF, GC, NVB, AS, DT, JPEM, HNW; Funding Acquisition: VAB, AS, VG, ESJS, JPEM; Investigation: IF, GC, NVB, AS, DT, JPEM; Methodology: VAB, CGF, ANM, VG, AS, ESJS, AG; Project Administration: VAB, ANM; Resources; VAB, ANM, CGF, ESJS, AG; Software: ANM, JPEM; Supervision: VAB, ANM, MJH, JPEM; Validation: IF, GC, NVB, AS; Writing – Original Draft Preparation: VAB, ANM; Writing – Review and Editing: CGF, ESJS, VG, JPEM, MJH

SUPPLEMENTARY MATERIAL

Supplementary material is linked to the online version of the paper at www.jidonline.org, and at https://doi.org/10.1016/j.jid.2022.04.028.

REFERENCES

Ahmed MI, Alam M, Emelianov VU, Poterlowicz K, Patel A, Sharov AA, et al. MicroRNA-214 controls skin and hair follicle development by modulating the activity of the Wnt pathway. J Cell Biol 2014;207:549–67.

Aramillo Irizar P, Schäuble S, Esser D, Groth M, Frahm C, Priebe S, et al. Transcriptomic alterations during ageing reflect the shift from cancer to degenerative diseases in the elderly [published correction appears in Nat Commun 2019;10:2459]. Nat Commun 2018;9:327.

Assabban A, Dubois-Vedrenne I, Van Maele L, Salcedo R, Snyder BL, Zhou L, et al. Tristetraprolin expression by keratinocytes protects against skin carcinogenesis. JCI Insight 2021;6:e140669.

Balasubramanian S, Ahmad N, Mukhtar H. Upregulation of E2F transcription factors in chemically induced mouse skin tumors. Int J Oncol 1999;15:387–90.

Barron CC, Bilan PJ, Tsakiridis T, Tsiani E. Facilitative glucose transporters: implications for cancer detection, prognosis and treatment. Metabolism 2016;65:124–39.

Barth E, Srivastava A, Stojiljkovic M, Frahm C, Axer H, Witte OW, et al. Conserved aging-related signatures of senescence and inflammation in different tissues and species. Aging (Albany NY) 2019;11:8556–72.

Bonnans C, Chou J, Werb Z. Remodelling the extracellular matrix in development and disease. Nat Rev Mol Cell Biol 2014;15:786–801.

Botchkarev VA. The molecular revolution in cutaneous biology: chromosomal territories, higher-order chromatin remodeling, and the control of gene expression in keratinocytes. J Invest Dermatol 2017;137:e93–9.

Botchkarev VA, Botchkarev NV, Albers KM, van der Veen C, Lewin GR, Paus R. Neurotrophin-3 involvement in the regulation of hair follicle morphogenesis. J Invest Dermatol 1998;111:279–85.

Botchkarev VA, Botchkareva NV, Roth W, Nakamura M, Chen LH, Herzog W, et al. Noggin is a mesenchymally derived stimulator of hair-follicle induction. Nat Cell Biol 1999;1:158–64.

Botchkarev VA, Flores ER. p53/p63/p73 in the epidermis in health and disease. Cold Spring Harb Perspect Med 2014;4:a015248.

Botchkarev VA, Gdula MR, Mardaryev AN, Sharov AA, Fessing MY. Epigenetic regulation of gene expression in keratinocytes. J Invest Dermatol 2012;132:2505–21.

Botchkareva NV, Botchkarev VA, Chen LH, Lindner G, Paus R. A role for p75 neurotrophin receptor in the control of hair follicle morphogenesis. Dev Biol 1999;216:135–53.

Braude S, Holtze S, Begall S, Brenmoehl J, Burda H, Dammann P, et al. Surprisingly long survival of premature conclusions about naked mole-rat biology. Biol Rev Camb Philos Soc 2021;96:376–93.

Brohus M, Gorbunova V, Faulkes CG, Overgaard MT, Conover CA. The insulin-like growth factor system in the long-lived naked mole-rat. PLoS One 2015;10:e0145587.

Buccitelli C, Selbach M. mRNAs, proteins and the emerging principles of gene expression control. Nat Rev Genet 2020;21:630–44.

Buffenstein R. The naked mole-rat: a new long-living model for human aging research. J Gerontol A Biol Sci Med Sci 2005;60:1369–77.

Buffenstein R, Amoroso V, Andziak B, Avdieiev S, Azpurua J, Barker AJ, et al. The naked truth: a comprehensive clarification and classification of current 'myths' in naked mole-rat biology. Biol Rev Camb Philos Soc 2022;97: 115–40.

Chuong CM, Nickoloff BJ, Elias PM, Goldsmith LA, Macher E, Maderson PA, et al. What is the 'true' function of skin? Exp Dermatol 2002;11:159–87.

Cole MA, Quan T, Voorhees JJ, Fisher GJ. Extracellular matrix regulation of fibroblast function: redefining our perspective on skin aging. J Cell Commun Signal 2018;12:35–43.

Crosara KTB, Moffa EB, Xiao Y, Siqueira WL. Merging in-silico and in vitro salivary protein complex partners using the STRING database: A tutorial. J Proteomics 2018;171:87–94.

Daly TJ, Buffenstein R. Skin morphology and its role in thermoregulation in mole-rats, Heterocephalus glaber and Cryptomys hottentotus. J Anat 1998;193:495–502.

Dammann P. Slow aging in mammals-Lessons from African mole-rats and bats. Semin Cell Dev Biol 2017;70:154–63.

Del Marmol D, Holtze S, Kichler N, Sahm A, Bihin B, Bourguignon V, et al. Abundance and size of hyaluronan in naked mole-rat tissues and plasma. Sci Rep 2021;11:7951.

Delaney MA, Nagy L, Kinsel MJ, Treuting PM. Spontaneous histologic lesions of the adult naked mole rat (Heterocephalus glaber): a retrospective survey of lesions in a zoo population. Vet Pathol 2013;50: 607–21.

Dimri GP, Lee X, Basile G, Acosta M, Scott G, Roskelley C, et al. A biomarker that identifies senescent human cells in culture and in aging skin in vivo. Proc Natl Acad Sci USA 1995;92:9363–7.

Evdokimov A, Kutuzov M, Petruseva I, Lukjanchikova N, Kashina E, Kolova E, et al. Naked mole rat cells display more efficient excision repair than mouse cells. Aging (Albany NY) 2018;10:1454–73.

Fessing MY, Mardaryev AN, Gdula MR, Sharov AA, Sharova TY, Rapisarda V, et al. p63 regulates Satb1 to control tissue-specific chromatin remodeling during development of the epidermis. J Cell Biol 2011;194:825–39.

Ge Y, Miao Y, Gur-Cohen S, Gomez N, Yang H, Nikolova M, et al. The aging skin microenvironment dictates stem cell behavior. Proc Natl Acad Sci USA 2020;117:5339–50.

Gladyshev VN, Zhang G, Wang J. The naked mole rat genome: understanding aging through genome analysis. Aging (Albany NY) 2011;3:1124.

Gorbunova V, Seluanov A, Zhang Z, Gladyshev VN, Vijg J. Comparative genetics of longevity and cancer: insights from long-lived rodents. Nat Rev Genet 2014;15:531–40.

Gunin AG, Petrov VV, Golubtzova NN, Vasilieva OV, Kornilova NK. Age-related changes in angiogenesis in human dermis. Exp Gerontol 2014;55: 143–51.

He B, Zhu R, Yang H, Lu Q, Wang W, Song L, et al. Assessing the impact of data preprocessing on analyzing next generation sequencing data. Front Bioeng Biotechnol 2020;8:817.

Horvath S, Haghani A, Macoretta N, Ablaeva J, Zoller JA, Li CZ, et al. DNA methylation clocks tick in naked mole rats but queens age more slowly than nonbreeders. Nat Aging 2022;2:46–59.

Jenkins BA, Fontecilla NM, Lu CP, Fuchs E, Lumpkin EA. The cellular basis of mechanosensory Merkel-cell innervation during development. ELife 2019;8:e42633.

Joly-Tonetti N, Wibawa JI, Bell M, Tobin D. Melanin fate in the human epidermis: a reassessment of how best to detect and analyse histologically. Exp Dermatol 2016;25:501–4.

Keyes BE, Segal JP, Heller E, Lien WH, Chang CY, Guo X, et al. Nfatc1 orchestrates aging in hair follicle stem cells. Proc Natl Acad Sci USA 2013;110:E4950–9.

Kim EB, Fang X, Fushan AA, Huang Z, Lobanov AV, Han L, et al. Genome sequencing reveals insights into physiology and longevity of the naked mole rat. Nature 2011;479:223–7.

Koster MI, Dai D, Roop DR. Conflicting roles for p63 in skin development and carcinogenesis. Cell Cycle 2007;6:269–73.

Kouwenhoven EN, Oti M, Niehues H, van Heeringen SJ, Schalkwijk J, Stunnenberg HG, et al. Transcription factor p63 bookmarks and regulates dynamic enhancers during epidermal differentiation. EMBO Rep 2015;16: 863–78.

Kulaberoglu Y, Bhushan B, Hadi F, Chakrabarti S, Khaled WT, Rankin KS, et al. The material properties of naked mole-rat hyaluronan. Sci Rep 2019;9:6632.

Langton AK, Graham HK, Watson RE. Diverse methodologies for assessing photoaged skin. Br J Dermatol 2016;174:487–8.

Langton AK, Sherratt MJ, Griffiths CE, Watson RE. A new wrinkle on old skin: the role of elastic fibres in skin ageing. Int J Cosmet Sci 2010;32:330–9.

Larsen SB, Cowley CJ, Fuchs E. Epithelial cells: liaisons of immunity. Curr Opin Immunol 2020;62:45–53.

Lewis DA, Travers JB, Somani AK, Spandau DF. The IGF-1/IGF-1R signaling axis in the skin: a new role for the dermis in aging-associated skin cancer. Oncogene 2010;29:1475–85.

Liu N, Matsumura H, Kato T, Ichinose S, Takada A, Namiki T, et al. Stem cell competition orchestrates skin homeostasis and ageing. Nature 2019;568: 344–50.

Lowe R, Danson AF, Rakyan VK, Yildizoglu S, Saldmann F, Viltard M, et al. DNA methylation clocks as a predictor for ageing and age estimation in naked mole-rats. *Heterocephalus glaber*. Aging (Albany NY) 2020;12:4394–406.

MacRae SL, Zhang Q, Lemetre C, Seim I, Calder RB, Hoeijmakers J, et al. Comparative analysis of genome maintenance genes in naked mole rat, mouse, and human. Aging Cell 2015;14:288–91.

Mardaryev AN, Gdula MR, Yarker JL, Emelianov VU, Poterlowicz K, Sharov AA, et al. p63 and Brg1 control developmentally regulated higher-order chromatin remodelling at the epidermal differentiation complex locus in epidermal progenitor cells [published correction appears in Development 2014;141:3437]. Development 2014;141:101–11.

Mardaryev AN, Liu B, Rapisarda V, Poterlowicz K, Malashchuk I, Rudolf J, et al. Cbx4 maintains the epithelial lineage identity and cell proliferation in the developing stratified epithelium. J Cell Biol 2016;212:77–89.

Martins R, Lithgow GJ, Link W. Long live FOXO: unraveling the role of FOXO proteins in aging and longevity. Aging Cell 2016;15:196–207.

Menon GK, Catania KC, Crumrine D, Bradley C, Mauldin EA. Unique features of the skin barrier in naked mole rats reflect adaptations to their fossorial habitat. J Morphol 2019;280:1871–80.

Menon GK, Kligman AM. Barrier functions of human skin: a holistic view. Skin Pharmacol Physiol 2009;22:178–89.

Müller-Röver S, Peters EJ, Botchkarev VA, Panteleyev A, Paus R. Distinct patterns of NCAM expression are associated with defined stages of murine hair follicle morphogenesis and regression. J Histochem Cytochem 1998;46:1401–10.

Parry A, Rulands S, Reik W. Active turnover of DNA methylation during cell fate decisions. Nat Rev Genet 2021;22:59–66.

Pilkington SM, Bulfone-Paus S, Griffiths CEM, Watson REB. Inflammaging and the skin. J Invest Dermatol 2021;141:1087–95.

Qu J, Yi G, Zhou H. p63 cooperates with CTCF to modulate chromatin architecture in skin keratinocytes. Epigenetics Chromatin 2019;12:31.

Raddatz G, Hagemann S, Aran D, Söhle J, Kulkarni PP, Kaderali L, et al. Aging is associated with highly defined epigenetic changes in the human epidermis. Epigenetics Chromatin 2013;6:36.

Rapisarda V, Malashchuk I, Asamaowei IE, Poterlowicz K, Fessing MY, Sharov AA, et al. p63 transcription factor regulates nuclear shape and expression of nuclear envelope-associated genes in epidermal keratinocytes. J Invest Dermatol 2017;137:2157–67.

Ressler S, Bartkova J, Niederegger H, Bartek J, Scharffetter-Kochanek K, Jansen-Dürr P, et al. p16INK4A is a robust in vivo biomarker of cellular aging in human skin. Aging Cell 2006;5:379–89.

Rittié L, Fisher GJ. UV-light-induced signal cascades and skin aging. Ageing Res Rev 2002;1:705–20.

Rittié L, Fisher GJ. Natural and sun-induced aging of human skin. Cold Spring Harb Perspect Med 2015;5:a015370.

Rodriguez KA, Valentine JM, Kramer DA, Gelfond JA, Kristan DM, Nevo E, et al. Determinants of rodent longevity in the chaperone-protein degradation network. Cell Stress Chaperones 2016;21:453–66.

Rognoni E, Watt FM. Skin cell heterogeneity in development, wound healing, and cancer. Trends Cell Biol 2018;28:709–22.

Rood BR, Leprince D. Deciphering HIC1 control pathways to reveal new avenues in cancer therapeutics. Expert Opin Ther Targets 2013;17:811–27.

Rosset C, Netto CBO, Ashton-Prolla P. TSC1 and TSC2 gene mutations and their implications for treatment in tuberous sclerosis Complex: a review. Genet Mol Biol 2017;40:69–79.

Savina A, Jaffredo T, Saldmann F, Faulkes CG, Moguelet P, Leroy C, et al. Single-cell transcriptomics reveals age-resistant maintenance of cell identities, stem cell compartments and differentiation trajectories in long-lived naked mole-rats skin. Aging 2022;14:3728–56.

Seluanov A, Gladyshev VN, Vijg J, Gorbunova V. Mechanisms of cancer resistance in long-lived mammals. Nat Rev Cancer 2018;18:433–41.

Sharov AA, Li GZ, Palkina TN, Sharova TY, Gilchrest BA, Botchkarev VA. Fas and c-kit are involved in the control of hair follicle melanocyte apoptosis and migration in chemotherapy-induced hair loss. J Invest Dermatol 2003;120:27–35.

Shebzukhov Y, Holtze S, Hirseland H, Schäfer H, Radbruch A, Hildebrandt T, et al. Identification of cross-reactive antibodies for the detection of lymphocytes, myeloid cells and haematopoietic precursors in the naked mole rat. Eur J Immunol 2019;49:2103–10.

Slominski AT, Zmijewski MA, Skobowiat C, Zbytek B, Slominski RM, Steketee JD. Sensing the environment: regulation of local and global homeostasis by the skin's neuroendocrine system. Adv Anat Embryol Cell Biol 2012;212. v, vii, 1–115.

Smith ESJ, Park TJ, Lewin GR. Independent evolution of pain insensitivity in African mole-rats: origins and mechanisms. J Comp Physiol A Neuroethol Sens Neural Behav Physiol 2020;206:313–25.

Sondka Z, Bamford S, Cole CG, Ward SA, Dunham I, Forbes SA. The COSMIC Cancer Gene Census: describing genetic dysfunction across all human cancers. Nat Rev Cancer 2018;18:696–705.

Stacpoole PW. The pyruvate dehydrogenase complex as a therapeutic target for age-related diseases. Aging Cell 2012;11:371–7.

Su X, Paris M, Gi YJ, Tsai KY, Cho MS, Lin YL, et al. TAp63 prevents premature aging by promoting adult stem cell maintenance. Cell Stem Cell 2009;5:64–75.

Tacutu R, Thornton D, Johnson E, Budovsky A, Barardo D, Craig T, et al. Human Ageing Genomic Resources: new and updated databases. Nucleic Acids Res 2018;46:D1083–90.

Takasugi M, Firsanov D, Tombline G, Ning H, Ablaeva J, Seluanov A, et al. Naked mole-rat very-high-molecular-mass hyaluronan exhibits superior cytoprotective properties. Nat Commun 2020;11:2376.

Thigpen LW. Histology of the skin of a normally hairless rodent. J Mammal 1940;21:449–56.

Tian X, Azpurua J, Ke Z, Augereau A, Zhang ZD, Vijg J, et al. INK4 locus of the tumor-resistant rodent, the naked mole rat, expresses a functional p15/p16 hybrid isoform. Proc Natl Acad Sci USA 2015;112:1053–8.

Toutfaire M, Bauwens E, Debacq-Chainiaux F. The impact of cellular senescence in skin ageing: a notion of mosaic and therapeutic strategies. Biochem Pharmacol 2017;142:1–12.

Tucker R. The digging behavior and skin differentiations in Heterocephalus glaber. J Morphol 1981;168:51–71.

Victorelli S, Lagnado A, Halim J, Moore W, Talbot D, Barrett K, et al. Senescent human melanocytes drive skin ageing via paracrine telomere dysfunction. EMBO J 2019;38:e101982.

Waaijer ME, Gunn DA, Adams PD, Pawlikowski JS, Griffiths CE, van Heemst D, et al. P16INK4a positive cells in human skin are indicative of local elastic fiber morphology, facial wrinkling, and perceived age. J Gerontol A Biol Sci Med Sci 2016;71:1022–8.

Waaijer ME, Parish WE, Strongitharm BH, van Heemst D, Slagboom PE, de Craen AJ, et al. The number of p16INK4a positive cells in human skin reflects biological age. Aging Cell 2012;11:722–5.

Waaijer MEC, Gunn DA, van Heemst D, Slagboom PE, Sedivy JM, Dirks RW, et al. Do senescence markers correlate in vitro and in situ within individual human donors? Aging (Albany NY) 2018;10:278–89.

Watt B, van Niel G, Raposo G, Marks MS. PMEL: a pigment cell-specific model for functional amyloid formation. Pigment Cell Melanoma Res 2013;26:300–15.

Winkler GS. The mammalian anti-proliferative BTG/Tob protein family. J Cell Physiol 2010;222:66–72.

Yaar M, Eller MS, Gilchrest BA. Fifty years of skin aging. J Investig Dermatol Symp Proc 2002;7:51–8.

Zhao Y, Tyshkovskiy A, Muñoz-Espín D, Tian X, Serrano M, de Magalhaes JP, et al. Naked mole rats can undergo developmental, oncogene-induced and DNA damage-induced cellular senescence. Proc Natl Acad Sci USA 2018;115:1801–6.

SUPPLEMENTARY MATERIALS AND METHODS

Quantification of immunofluorescence intensity

Red or green fluorescent signal was collected from experimental tissues in RGB (red, green, and blue) format using the same exposure conditions. Regions of interest of distinct size within the epidermis or dermis were selected, and the corrected total cell fluorescence value was quantified using integrated density of the immunofluorescence against the area of the selected region and the mean gray value of the background. At least 10 ×40 images per group with exactly the same image acquisition parameters have been taken. Statistical analysis was performed using unpaired Student's *t*-test; differences were deemed significant if $P < 0.05$.

We used a complex approach to avoid significant errors in the quantification of fluorescence intensity as follows:

1. To avoid the errors derived from the UV source, the fluorescence bulbs were regularly replaced before reaching their maximum lifespan by a qualified technician.
2. To minimize the issue related to the fading of fluorescent dyes, we used Alexa-coupled secondary antibodies. Alexa dyes are proven to be more photostable than their commonly used fluorophores (Panchuk-Voloshina et al., 1999). Maintaining the same exposure conditions that were set to avoid oversaturation and undersaturation, an area of imaging was exposed only once for a very short time required to capture the image. Acquisition of images for each immunofluorescence protocol (each antibody), including both age groups, was performed by the same person during one imaging session. Monochrome grayscale images were acquired with Qimaging Retiga Exi Aqua Mono camera, which supports low light fluorescent imaging, with enhanced sensitivity, high resolution, and broad spectral response (https://www.mediacy.com/support/imagepro/hardware). For illustration purposes, each grayscale image channel was pseudocolored and merged to produce colored images in RGB format with the Image Pro Insight 9.0 software.
3. For image analysis, background correction for total fluorescence correction was performed. Analysis of pixel intensity values was done on raw flat-field grayscale 16-bit TIFF images that preserve the linear relationship between the photons and image intensity values.

RNA extraction and RNA-sequencing analyses

For RNA sequencing, approximately 10 μg of total RNA was used to remove ribosomal RNA according to the manuscript of the Epicentre Ribo-Zero Gold Kit (Illumina, San Diego, CA). After purification, the ribo-minus RNA fractions were fragmented into small pieces using divalent cations under elevated temperatures. Then, the cleaved RNA fragments were reverse transcribed to create the final cDNA library in accordance with a strand-specific library preparation by the deoxyuridine triphosphate method. The average insert size for the paired-end libraries was 300 ± 50 bp. The pair-end 2 × 150 bp sequencing was performed on an Illumina Hiseq 4000 platform in the LC Sciences (Houston, TX).

Bioinformatics and protein–protein interaction network analyses

The bioinformatics analysis of the RNA-sequencing data was performed by the LC Sciences. First, Cutadapt (Martin, 2011) and Perl scripts were used to remove the reads that contained adaptor contamination, low-quality bases, and undetermined bases. Then, sequence quality was verified using FastQC (http://www.bioinformatics.babraham.ac.uk/projects/fastqc/). Bowtie2 (Langmead and Salzberg, 2012) and Tophat2 (Kim et al., 2013) were used to map reads to the genome of *Heterocephalus glaber* (https://useast.ensembl.org/Heterocephalus_glaber_female/Info/Index). The differentially expressed mRNAs were selected with $\log_2$ (fold change) > 1 or $\log_2$ (fold change) < −1 and with parametric F-test comparing nested linear models ($P < 0.05$) by R package Ballgown. Ballgown was used to generate a list and heatmaps of differentially expressed genes, and in-house generated Perl scripts (LC Science) were used for Gene Ontology and Kyoto Encyclopedia of Genes and Genomes pathway enrichment analyses. In addition, to cluster differentially expressed genes into different functional groups, the Qiagen Ingenuity Pathway Analysis (Qiagen, Hilden, Germany) was used (https://digitalinsights.qiagen.com/products-overview/discovery-insights-portfolio/analysis-and-visualization/qiagen-ipa/) as a general platform, and skin-relevant functional gene subcategories were manually organized accordingly to previously published data (Sharov et al., 2009, 2006). In addition, for each time interval, the significantly differentially expressed genes were input into Human Ageing Genome Resource (https://genomics.senescence.info/) or Cancer Gene Census (https://cancer.sanger.ac.uk/census) databases. In addition, ClusterProfiler R Package was used to identify Kyoto Encyclopedia of Genes and Genomes Pathway enrichment and Gene Ontology functional term enrichment for each of the gene sets.

To predict the functional interaction of proteins encoded by differentially expressed genes in young and aged naked mole rats, the STRING (search tool for retrieval of interacting genes) (https://string-db.org, vision 11.0) database was employed. Active interaction sources, including text mining, experiments, databases, and coexpression as well as species limited to *Heterocephalus glaber* and an interaction score- > 0.4 were applied to construct the protein–protein interaction networks. Gene Ontology and Kyoto Encyclopedia of Genes and Genomes pathways were selected with the threshold of adjusted $P < 0.05$.

SUPPLEMENTARY REFERENCES

Aramillo Irizar P, Schäuble S, Esser D, Groth M, Frahm C, Priebe S, et al. Transcriptomic alterations during ageing reflect the shift from cancer to degenerative diseases in the elderly [published correction appears in Nat Commun 2019;10:2459. Nat Commun 2018;9:327.

Barth E, Srivastava A, Stojiljkovic M, Frahm C, Axer H, Witte OW, et al. Conserved aging-related signatures of senescence and inflammation in different tissues and species. Aging (Albany NY) 2019;11:8556–72.

Kim D, Pertea G, Trapnell C, Pimentel H, Kelley R, Salzberg SL. TopHat2: accurate alignment of transcriptomes in the presence of insertions, deletions and gene fusions. Genome Biol 2013;14:R36.

Langmead B, Salzberg SL. Fast gapped-read alignment with Bowtie 2. Nat Methods 2012;4:357–9.

Martin M. Cutadapt Removes Adapter Sequences from High-Throughput Sequencing Reads. EMBnet Journal 2011;17:10–2.

Panchuk-Voloshina N, Haugland RP, Bishop-Stewart J, Bhalgat MK, Millard PJ, Mao F, et al. Alexa dyes, a series of new fluorescent dyes that yield exceptionally bright, photostable conjugates. J Histochem Cytochem 1999;47:1179–88.

Sharov A, Sharova TY, Mardaryev AN, Tommasi di Vignano A, Atoyan R, Weiner L, et al. Bone morphogenetic protein signaling regulates the size of hair follicles and modulates the expression of cell cycle-associated genes. Proc Natl Acad Sci U S A 2006;103:18166–71.

Sharov AA, Mardaryev AN, Sharova TY, Grachtchouk M, Atoyan R, Byers HR, et al. Bone morphogenetic protein antagonist noggin promotes skin tumorigenesis via stimulation of the Wnt and Shh signaling pathways. Am J Pathol 2009;175:1303–14.

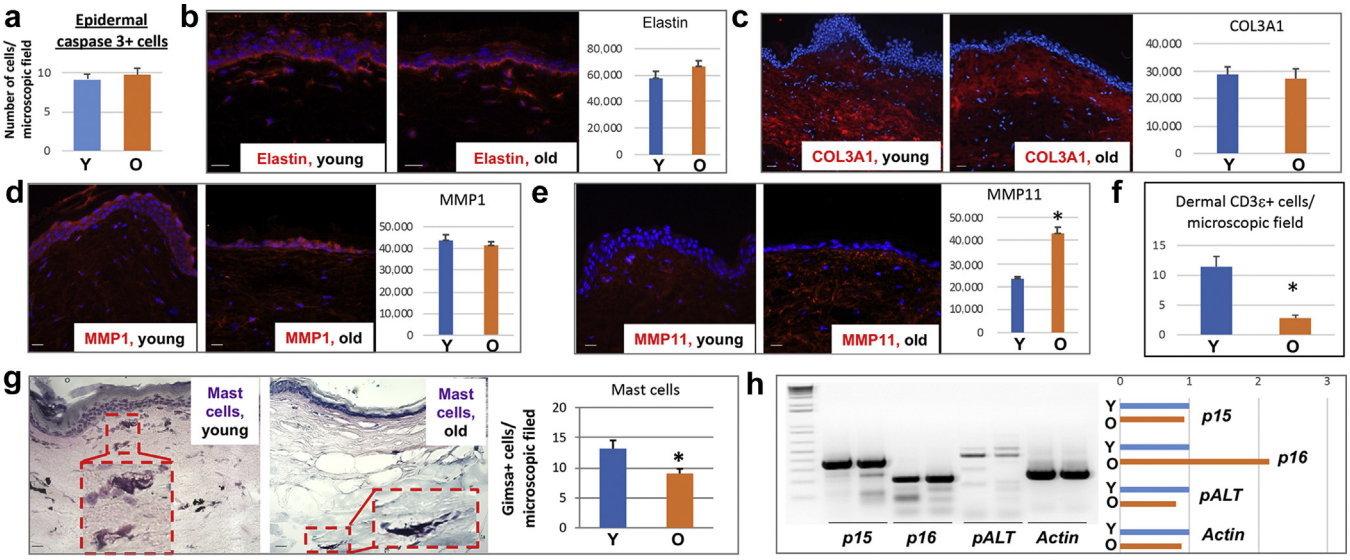

Supplementary Figure S1. Characterization of young and old NMR skin. (a) A quantitative analysis of active caspase 3–positive cells: no difference in expression levels between the epidermis of young and old NMRs. **(b)** COL3A1 expression in the upper dermis of old NMRs: no difference in total expression levels between young and old animals. **(c)** Distribution of dermal elastic fibers and elastin expression levels are similar between the dermis of young and old animals. **(d)** Epidermal MMP1 expression with equal immunofluorescence intensity between young and old animals. **(e)** Marked increase of MMP11 immunofluorescence in the dermis of old NMRs compared with that of young animals. **(f)** A significant decrease in the number of CD3ε+ T cells in the dermis of aged NMR skin. **(g)** A significant decline in the number of mast cells in aged NMR skin as detected by Giemsa stain. **(h)** qRT-PCR: upregulation of $p16^{INK4a}$ in aged versus young full-thickness skin samples and similar levels of $p15^{INK4b}$ and $pALT^{INK4a/b}$ are seen in old and young skin. Data are expressed as mean ± SD. $^*P < 0.01$ with Student's *t*-test. Bars = 25 μm. Y denotes young animals, and O denotes old animals. A.u., arbitrary unit; MMP, matrix metalloproteinase; NMR, naked mole rat.

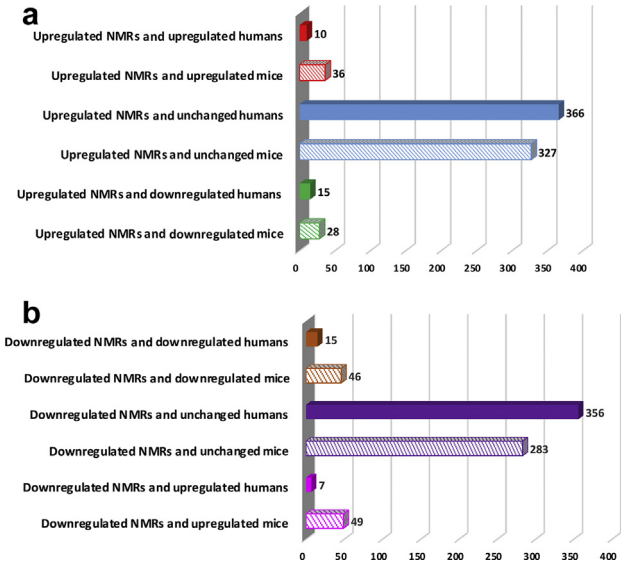

Supplementary Figure S2. The correlation of the age-associated changes in the NMR skin transcriptome to human or mouse skin aging. Age-associated transcriptome from NMR skin was compared with the transcriptome data from aged human and mouse skin obtained from publicly available datasets (Aramillo Irizar et al., 2018; Barth et al., 2019). **(a)** The number of genes upregulated during aging in the NMR skin showing similarities or differences in expression in comparison with those in human or mouse skin aging. **(a)** The number of genes downregulated during aging in the NMR skin showing the similarities or differences in expression in comparison with those in human or mouse skin aging. NMR, naked mole rat.

Supplementary Figure S3. Validation of the changes in the NMR skin aging transcriptome by immunofluorescence. (a–c) Significant increase of **(a)** CDKN1A, **(b)** BTG2, and **(c)** TOB1 immunofluorescence in the epidermis of aged NMR skin. Data are expressed as mean ± SD. $*P < 0.01$ with Student's *t*-test. Y denotes young animals, and O denotes old animals. Bars = 25 μm. A.u., arbitrary unit; NMR, naked mole rat.

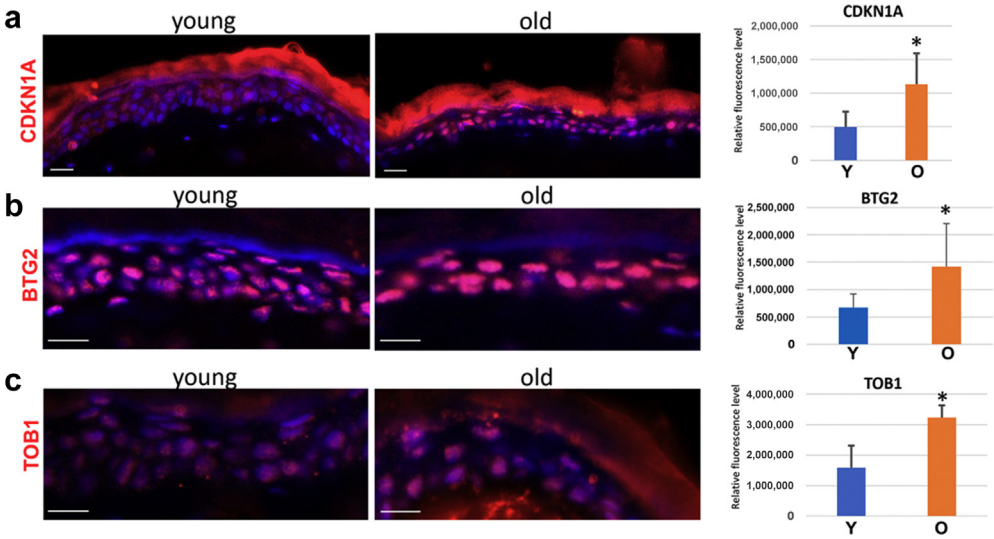

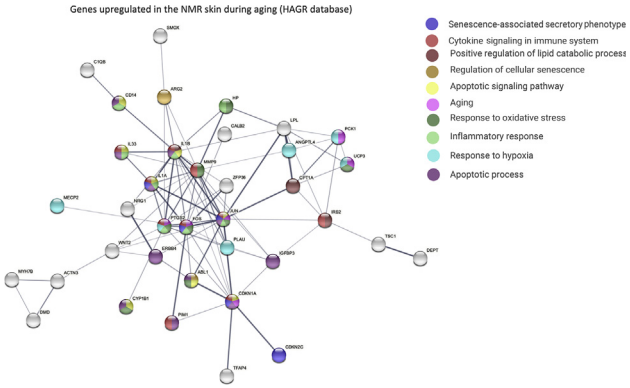

Supplementary Figure S4. The STRING protein–protein interaction network analysis showing the associations among the genes upregulated in the aged NMR skin and longevity-associated genes present in the HAGR database. Color nodes represent the proteins associated with the corresponding GO term and KEGG pathways, whereas the thickness of the network edges (links) shows the strength of data support used for the network reconstruction. GO, Gene Ontology; HAGR, Human Aging Genome Resource; KEGG, Kyoto Encyclopedia of Genes and Genomes; NMR, naked mole rat; STRING, search tool for retrieval of interacting genes.

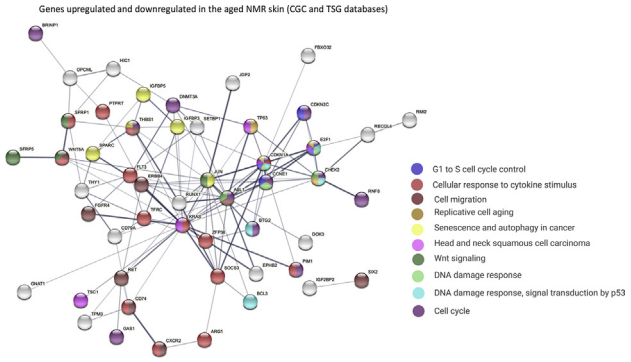

Supplementary Figure S6. The STRING protein–protein interaction network analysis showing the associations among the genes differentially expressed in the aged NMR skin and cancer-related/tumor suppressor genes present in CGC/TSGene databases. Color nodes represent the proteins associated with the corresponding GO term and KEGG pathways, whereas the thickness of the network edges (links) shows the strength of data support used for the network reconstruction. CGC, Cancer Gene Census; GO, Gene Ontology; KEGG, Kyoto Encyclopedia of Genes and Genomes; NMR, naked mole rat; STRING, search tool for retrieval of interacting genes; TSGene, Tumor Suppressor Genes.

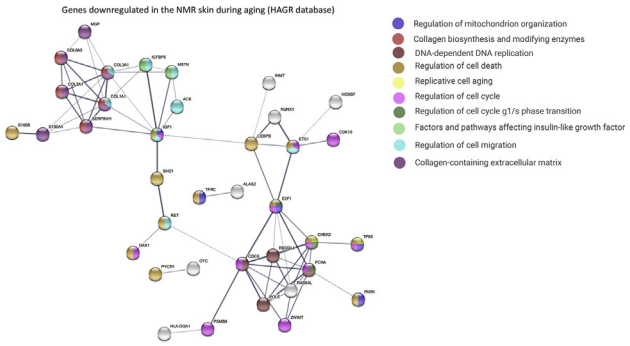

Supplementary Figure S5. The STRING protein–protein interaction network analysis showing the associations among the genes downregulated in the aged NMR skin and longevity-associated genes present in the HAGR database. Color nodes represent the proteins associated with the corresponding GO term and KEGG pathways, whereas the thickness of the network edges (links) shows the strength of data support used for the network reconstruction. GO, Gene Ontology; HAGR, Human Aging Genome Resource; KEGG, Kyoto Encyclopedia of Genes and Genomes; NMR, naked mole rat; STRING, search tool for retrieval of interacting genes.